

# Simulation of a Double Gate MOSFET through a hybrid quantum/classical model

Naoufel Ben Abdallah, María José Cáceres, José Antonio Carrillo,  
Francesco Vecil

PDEs in Engineering Nanoscience and Biology, Hammamet, May 2010

# Outline

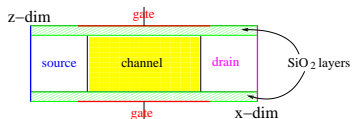
- 1 The model
  - Geometry
  - Mathematical model
- 2 Numerical methods for the Schrödinger-Poisson block
  - Iterative schemes
  - Solvers for Schrödinger and Poisson
- 3 Solvers for the BTE block
  - Adimensionalizations
  - Time discretization
  - Linear advection
  - PWENO interpolations
- 4 Experiments
  - Simplifying assumptions
  - Equilibria
  - Time-dependent simulations
  - Newton vs. Gummel
  - Plasma oscillations

# Outline

- 1 The model
  - Geometry
  - Mathematical model
- 2 Numerical methods for the Schrödinger-Poisson block
  - Iterative schemes
  - Solvers for Schrödinger and Poisson
- 3 Solvers for the BTE block
  - Adimensionalizations
  - Time discretization
  - Linear advection
  - PWENO interpolations
- 4 Experiments
  - Simplifying assumptions
  - Equilibria
  - Time-dependent simulations
  - Newton vs. Gummel
  - Plasma oscillations

# The model

We afford the simulation of a nanoscaled MOSFET.



## Dimensional coupling

$x$ -dimension is unconfined unlike  $z$ -dimension, therefore we adopt a different description:

- along  $x$ -dimension the electrons behave like **particles**, their movement being described by the Boltzmann Transport Equation;
- along  $z$ -dimension the electrons, confined in a potential well, behave like **waves**; the equilibrium being reached much faster than transport (quasi-static phenomenon), their state is given by the stationary-state Schrödinger equation.

# The model

## Subband decomposition

Due to the confinement, different *sub-bands* (another name for the **eigenvalues of the Schrödinger equation**) identify independent populations, which have to be transported for separate.

## Coupling between dimensions

Dimensions and subbands are coupled in the Poisson equation for the computation of the electrostatic field in the expression of the total density.

# The model

## Subband decomposition

Due to the confinement, different *sub-bands* (another name for the **eigenvalues of the Schrödinger equation**) identify independent populations, which have to be transported for separate.

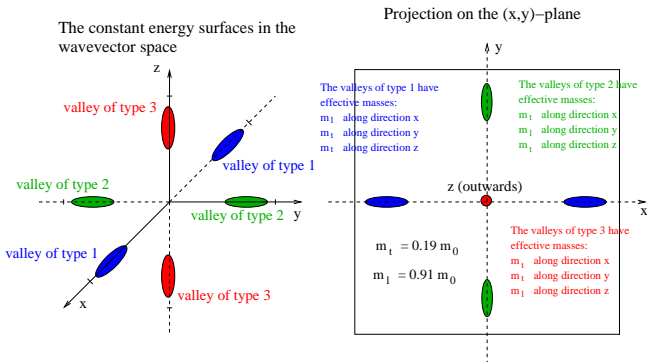
## Coupling between dimensions

Dimensions and subbands are coupled in the Poisson equation for the computation of the electrostatic field in the expression of the total density.

# Bandstructure

## The three valleys

The Si bandstructure presents six minima in the first Brillouin zone:



The axes of the ellipsoids are disposed along the  $x$ ,  $y$  and  $z$  axes of the reciprocal lattice. The three minima have the same value, therefore there is no gap.

# Bandstructure

## Coupling between subbands and valleys

The sub-bands as well as the valleys are coupled by the Poisson equation in the expression of the total density and, if the case, by the scattering operator.

## Non-parabolicity

The bandstructure around the three minima can be expanded following the Kane non-parabolic approximation ( $\nu$  indexes the valley):

$$\epsilon_{\nu}^{kin} = \frac{\hbar^2}{1 + \sqrt{1 + 2\tilde{\alpha}_{\nu}\hbar^2 \left( \frac{k_x^2}{m_{x,\nu}} + \frac{k_y^2}{m_{y,\nu}} \right)}} \left( \frac{k_x^2}{m_{x,\nu}} + \frac{k_y^2}{m_{y,\nu}} \right),$$

where  $m_{\{x,y,z\},\nu}$  are the axes of the ellipsoids (called *effective masses*) of the  $\nu^{\text{th}}$  valley along  $x$ ,  $y$  and  $z$  directions, and the  $\tilde{\alpha}_{\nu}$  are known as Kane dispersion factors.



# Bandstructure

## Coupling between subbands and valleys

The sub-bands as well as the valleys are coupled by the Poisson equation in the expression of the total density and, if the case, by the scattering operator.

## Non-parabolicity

The bandstructure around the three minima can be expanded following the Kane non-parabolic approximation ( $\nu$  indexes the valley):

$$\epsilon_{\nu}^{kin} = \frac{\hbar^2}{1 + \sqrt{1 + 2\tilde{\alpha}_{\nu}\hbar^2 \left( \frac{k_x^2}{m_{x,\nu}} + \frac{k_y^2}{m_{y,\nu}} \right)}} \left( \frac{k_x^2}{m_{x,\nu}} + \frac{k_y^2}{m_{y,\nu}} \right),$$

where  $m_{\{x,y,z\},\nu}$  are the axes of the ellipsoids (called *effective masses*) of the  $\nu^{\text{th}}$  valley along  $x$ ,  $y$  and  $z$  directions, and the  $\tilde{\alpha}_{\nu}$  are known as Kane dispersion factors.

# Outline

- 1 The model
  - Geometry
  - **Mathematical model**
- 2 Numerical methods for the Schrödinger-Poisson block
  - Iterative schemes
  - Solvers for Schrödinger and Poisson
- 3 Solvers for the BTE block
  - Adimensionalizations
  - Time discretization
  - Linear advection
  - PWENO interpolations
- 4 Experiments
  - Simplifying assumptions
  - Equilibria
  - Time-dependent simulations
  - Newton vs. Gummel
  - Plasma oscillations

# The model

## BTE

The Boltzmann Transport Equation (one for each band and for each valley) reads

$$\frac{\partial f_{\nu,p}}{\partial t} + \frac{1}{\hbar} \nabla_k \epsilon_{\nu}^{\text{kin}} \cdot \nabla_x f_{\nu,p} - \frac{1}{\hbar} \nabla_x \epsilon_{\nu,p}^{\text{pot}} \cdot \nabla_k f_{\nu,p} = \mathcal{Q}_{\nu,p}[f], \quad f_{\nu,p}(t=0) = \rho_{\nu,p}^{\text{eq}} M_{\nu}.$$

## Schrödinger-Poisson block

$$-\frac{\hbar^2}{2} \frac{d}{dz} \left[ \frac{1}{m_{z,\nu}} \frac{d\chi_{\nu,p}[V]}{dz} \right] - q(V + V_c) \chi_{\nu,p}[V] = \epsilon_{\nu,p}^{\text{pot}}[V] \chi_{\nu,p}[V]$$

$$\langle \chi_{\nu,p}[V], \chi_{\nu,p'}[V] \rangle = \delta_{p,p'}$$

$$-\text{div} [\epsilon_R \nabla V] = -\frac{q}{\epsilon_0} (N[V] - N_D)$$

$$N[V] = \sum_{\nu,p} \rho_{\nu,p} |\chi_{\nu,p}[V]|^2$$

These equations cannot be decoupled because we need the **eigenfunctions** to compute the potential (in the expression of the **total density**), and we need the potential to compute the eigenfunctions.

# The model

## BTE

The Boltzmann Transport Equation (one for each band and for each valley) reads

$$\frac{\partial f_{\nu,p}}{\partial t} + \frac{1}{\hbar} \nabla_k \epsilon_{\nu}^{\text{kin}} \cdot \nabla_x f_{\nu,p} - \frac{1}{\hbar} \nabla_x \epsilon_{\nu,p}^{\text{pot}} \cdot \nabla_k f_{\nu,p} = \mathcal{Q}_{\nu,p}[f], \quad f_{\nu,p}(t=0) = \rho_{\nu,p}^{\text{eq}} M_{\nu}.$$

## Schrödinger-Poisson block

$$-\frac{\hbar^2}{2} \frac{d}{dz} \left[ \frac{1}{m_{z,\nu}} \frac{d\chi_{\nu,p}[V]}{dz} \right] - q(V + V_c) \chi_{\nu,p}[V] = \epsilon_{\nu,p}^{\text{pot}}[V] \chi_{\nu,p}[V]$$

$$\langle \chi_{\nu,p}[V], \chi_{\nu,p'}[V] \rangle = \delta_{p,p'}$$

$$-\text{div} [\epsilon_R \nabla V] = -\frac{q}{\epsilon_0} (N[V] - N_D)$$

$$N[V] = \sum_{\nu,p} \rho_{\nu,p} |\chi_{\nu,p}[V]|^2$$

These equations cannot be decoupled because we need the **eigenfunctions** to compute the potential (in the expression of the **total density**), and we need the potential to compute the eigenfunctions.

# The model

## The collision operator

The collision operator takes into account the phonon scattering mechanism. It reads

$$\mathcal{Q}_{\nu,p}[f] = \sum_s \mathcal{Q}_{\nu,p}^s[f]$$

$$\mathcal{Q}_{\nu,p}^s[f] = \sum_{\nu',p'} \int_{\mathbb{R}^2} [S_{(\nu',p',k') \rightarrow (\nu,p,k)}^s f_{\nu',p'}(k') - S_{(\nu,p,k) \rightarrow (\nu',p',k')}^s f_{\nu,p}(k)] dk' :$$

every  $S^s$  represents a different interaction.

## Structure of the $S^s$

The missing dimension of the wave-vector  $k \in \mathbb{R}^2$ , instead of  $k \in \mathbb{R}^3$ , is replaced by an overlap integral  $W_{(\nu,p),(\nu',p')}$ :

$$S_{(\nu,p,k) \rightarrow (\nu',p',k')}^s = C_{\nu \rightarrow \nu'} \frac{1}{W_{(\nu,p),(\nu',p')}} \delta(\epsilon_{\nu',p'}^{\text{tot}}(k') - \epsilon_{\nu,p}^{\text{tot}}(k) \pm \text{some energy})$$

$$\frac{1}{W_{(\nu,p),(\nu',p')}} = \int_0^{l_z} |\chi_{\nu,p}|^2 |\chi_{\nu',p'}|^2 dz, \quad [W] = m.$$

# The model

## The collision operator

The collision operator takes into account the phonon scattering mechanism. It reads

$$\mathcal{Q}_{\nu,p}[f] = \sum_s \mathcal{Q}_{\nu,p}^s[f]$$

$$\mathcal{Q}_{\nu,p}^s[f] = \sum_{\nu',p'} \int_{\mathbb{R}^2} [S_{(\nu',p',k') \rightarrow (\nu,p,k)}^s f_{\nu',p'}(k') - S_{(\nu,p,k) \rightarrow (\nu',p',k')}^s f_{\nu,p}(k)] dk' :$$

every  $S^s$  represents a different interaction.

## Structure of the $S^s$

The missing dimension of the wave-vector  $k \in \mathbb{R}^2$ , instead of  $k \in \mathbb{R}^3$ , is replaced by an overlap integral  $W_{(\nu,p),(\nu',p')}$ :

$$S_{(\nu,p,k) \rightarrow (\nu',p',k')}^s = C_{\nu \rightarrow \nu'} \frac{1}{W_{(\nu,p),(\nu',p')}} \delta(\epsilon_{\nu',p'}^{\text{tot}}(k') - \epsilon_{\nu,p}^{\text{tot}}(k) \pm \text{some energy})$$

$$\frac{1}{W_{(\nu,p),(\nu',p')}} = \int_0^{l_z} |\chi_{\nu,p}|^2 |\chi_{\nu',p'}|^2 dz, \quad [W] = m.$$



# Outline

- 1 The model
  - Geometry
  - Mathematical model
- 2 Numerical methods for the Schrödinger-Poisson block
  - **Iterative schemes**
  - Solvers for Schrödinger and Poisson
- 3 Solvers for the BTE block
  - Adimensionalizations
  - Time discretization
  - Linear advection
  - PWENO interpolations
- 4 Experiments
  - Simplifying assumptions
  - Equilibria
  - Time-dependent simulations
  - Newton vs. Gummel
  - Plasma oscillations



# The Newton scheme

## The functional

Solving the Schrödinger-Poisson block

$$-\frac{\hbar^2}{2} \frac{d}{dz} \left[ \frac{1}{m_{z,\nu}} \frac{d\chi_{\nu,p}[V]}{dz} \right] - q(V + V_c) \chi_{\nu,p}[V] = \epsilon_{\nu,p}^{pot}[V] \chi_{\nu,p}[V]$$

$$-\text{div} [\epsilon_R \nabla V] = -\frac{q}{\epsilon_0} (N[V] - N_D)$$

is equivalent to minimizing, under the constraints of the Schrödinger equation, the functional  $P[V]$

$$P[V] = -\text{div} (\epsilon_R \nabla V) + \frac{q}{\epsilon_0} (N[V] - N_D),$$

## The scheme

which is achieved by means of a Newton-Raphson iterative scheme

$$dP(V^{old}, V^{new} - V^{old}) = -P[V^{old}].$$

# The Newton scheme

## The functional

Solving the Schrödinger-Poisson block

$$-\frac{\hbar^2}{2} \frac{d}{dz} \left[ \frac{1}{m_{z,\nu}} \frac{d\chi_{\nu,p}[V]}{dz} \right] - q(V + V_c) \chi_{\nu,p}[V] = \epsilon_{\nu,p}^{pot}[V] \chi_{\nu,p}[V]$$

$$-\text{div} [\epsilon_R \nabla V] = -\frac{q}{\epsilon_0} (N[V] - N_D)$$

is equivalent to minimizing, under the constraints of the Schrödinger equation, the functional  $P[V]$

$$P[V] = -\text{div} (\epsilon_R \nabla V) + \frac{q}{\epsilon_0} (N[V] - N_D),$$

## The scheme

which is achieved by means of a Newton-Raphson iterative scheme

$$dP(V^{old}, V^{new} - V^{old}) = -P[V^{old}].$$

# The iterations

## Derivatives

The Gâteaux-derivatives of the eigenproperties are needed:

$$d\epsilon_{\nu,p}(V, U) = -q \int U(\zeta) |\chi_{\nu,p}[V](\zeta)|^2 d\zeta$$

$$d\chi_{\nu,p}(V, U) = -q \sum_{p' \neq p} \frac{\int U(\zeta) \chi_{\nu,p}[V](\zeta) \chi_{\nu,p'}[V](\zeta) d\zeta}{\epsilon_{\nu,p}[V] - \epsilon_{\nu,p'}[V]} \chi_{\nu,p'}[V](z).$$

## Iterations

After computing the Gâteaux-derivative of the density and developing calculations, we are led to a Poisson-like equation

$$-\operatorname{div}(\epsilon_R \nabla V^{new}) + \int_0^{l_z} \mathcal{A}[V^{old}](z, \zeta) V^{new}(\zeta) d\zeta$$

$$= -\frac{q}{\epsilon_0} (N[V^{old}] - N_D) + \int_0^{l_z} \mathcal{A}[V^{old}](z, \zeta) V^{old}(\zeta) d\zeta,$$

where  $\mathcal{A}[V]$  is essentially the Gâteaux-derivative of the functional  $P[V]$ .

# The iterations

## Derivatives

The Gâteaux-derivatives of the eigenproperties are needed:

$$d\epsilon_{\nu,p}(V, U) = -q \int U(\zeta) |\chi_{\nu,p}[V](\zeta)|^2 d\zeta$$

$$d\chi_{\nu,p}(V, U) = -q \sum_{p' \neq p} \frac{\int U(\zeta) \chi_{\nu,p}[V](\zeta) \chi_{\nu,p'}[V](\zeta) d\zeta}{\epsilon_{\nu,p}[V] - \epsilon_{\nu,p'}[V]} \chi_{\nu,p'}[V](z).$$

## Iterations

After computing the Gâteaux-derivative of the density and developing calculations, we are led to a Poisson-like equation

$$-\operatorname{div}(\epsilon_R \nabla V^{new}) + \int_0^{l_z} \mathcal{A}[V^{old}](z, \zeta) V^{new}(\zeta) d\zeta$$

$$= -\frac{q}{\epsilon_0} (N[V^{old}] - N_D) + \int_0^{l_z} \mathcal{A}[V^{old}](z, \zeta) V^{old}(\zeta) d\zeta,$$

where  $\mathcal{A}[V]$  is essentially the Gâteaux-derivative of the functional  $P[V]$ .

# The Gummel scheme

## The iteration

Solving the Schrödinger-Poisson block

$$\begin{aligned}
 & -\operatorname{div}(\varepsilon_R \nabla V^{new}) + \frac{q}{\varepsilon_0} N[V^{old}] \frac{q}{k_B T_L} V^{new} \\
 = & -\frac{q}{\varepsilon_0} (N[V^{old}] - N_D) + \frac{q}{\varepsilon_0} N[V^{old}] \frac{q}{k_B T_L} V^{old},
 \end{aligned}$$

## Comparison with Newton

We here repeat the Newton iteration:

$$\begin{aligned}
 & -\operatorname{div}(\varepsilon_R \nabla V^{new}) + \int_0^{l_z} \mathcal{A}[V^{old}](z, \zeta) V^{new}(\zeta) d\zeta \\
 = & -\frac{q}{\varepsilon_0} (N[V^{old}] - N_D) + \int_0^{l_z} \mathcal{A}[V^{old}](z, \zeta) V^{old}(\zeta) d\zeta,
 \end{aligned}$$

# The Gummel scheme

## The iteration

Solving the Schrödinger-Poisson block

$$\begin{aligned} & -\operatorname{div}(\varepsilon_R \nabla V^{new}) + \frac{q}{\varepsilon_0} N[V^{old}] \frac{q}{k_B T_L} V^{new} \\ = & -\frac{q}{\varepsilon_0} (N[V^{old}] - N_D) + \frac{q}{\varepsilon_0} N[V^{old}] \frac{q}{k_B T_L} V^{old}, \end{aligned}$$

## Comparison with Newton

We here repeat the Newton iteration:

$$\begin{aligned} & -\operatorname{div}(\varepsilon_R \nabla V^{new}) + \int_0^{l_z} \mathcal{A}[V^{old}](z, \zeta) V^{new}(\zeta) d\zeta \\ = & -\frac{q}{\varepsilon_0} (N[V^{old}] - N_D) + \int_0^{l_z} \mathcal{A}[V^{old}](z, \zeta) V^{old}(\zeta) d\zeta, \end{aligned}$$



# Outline

- 1 The model
  - Geometry
  - Mathematical model
- 2 Numerical methods for the Schrödinger-Poisson block
  - Iterative schemes
  - Solvers for Schrödinger and Poisson
- 3 Solvers for the BTE block
  - Adimensionalizations
  - Time discretization
  - Linear advection
  - PWENO interpolations
- 4 Experiments
  - Simplifying assumptions
  - Equilibria
  - Time-dependent simulations
  - Newton vs. Gummel
  - Plasma oscillations



# Numerical methods

We need to solve the Schrödinger eigenvalue problem and Poisson equations.

## The Schrödinger equation

Equation

$$-\frac{\hbar^2}{2} \frac{d}{dz} \left[ \frac{1}{m_{z,\nu}} \frac{d\chi_{\nu,p}}{dz} \right] - q(V + V_c) \chi_{\nu,p} = \epsilon_{\nu,p} \chi_{\nu,p}$$

is discretized by alternate finite differences for the derivatives then the symmetric matrix is diagonalized by a LAPACK routine called DSTEQR.

## The Poisson equation

We need to solve equations like

$$-\text{div} [\epsilon_R \nabla V] + \int_0^{t_z} \mathcal{A}(z, \zeta) V(\zeta) d\zeta = \mathcal{B}(z).$$

The derivatives are discretized by finite differences in alternate directions, the integral is computed via trapezoid rule and the linear system (full) is solved by means of a LAPACK routine called DGESV.

# Numerical methods

We need to solve the Schrödinger eigenvalue problem and Poisson equations.

## The Schrödinger equation

Equation

$$-\frac{\hbar^2}{2} \frac{d}{dz} \left[ \frac{1}{m_{z,\nu}} \frac{d\chi_{\nu,p}}{dz} \right] - q(V + V_c) \chi_{\nu,p} = \epsilon_{\nu,p} \chi_{\nu,p}$$

is discretized by alternate finite differences for the derivatives then the symmetric matrix is diagonalized by a LAPACK routine called DSTEQR.

## The Poisson equation

We need to solve equations like

$$-\text{div} [\epsilon_R \nabla V] + \int_0^{t_z} \mathcal{A}(z, \zeta) V(\zeta) d\zeta = \mathcal{B}(z).$$

The derivatives are discretized by finite differences in alternate directions, the integral is computed via trapezoid rule and the linear system (full) is solved by means of a LAPACK routine called DGESV.

# Numerical methods

We need to solve the Schrödinger eigenvalue problem and Poisson equations.

## The Schrödinger equation

Equation

$$-\frac{\hbar^2}{2} \frac{d}{dz} \left[ \frac{1}{m_{z,\nu}} \frac{d\chi_{\nu,p}}{dz} \right] - q(V + V_c) \chi_{\nu,p} = \epsilon_{\nu,p} \chi_{\nu,p}$$

is discretized by alternate finite differences for the derivatives then the symmetric matrix is diagonalized by a LAPACK routine called DSTEQR.

## The Poisson equation

We need to solve equations like

$$-\text{div} [\epsilon_R \nabla V] + \int_0^{l_z} \mathcal{A}(z, \zeta) V(\zeta) d\zeta = \mathcal{B}(z).$$

The derivatives are discretized by finite differences in alternate directions, the integral is computed via trapezoid rule and the linear system (full) is solved by means of a LAPACK routine called DGESV.

# Outline

- 1 The model
  - Geometry
  - Mathematical model
- 2 Numerical methods for the Schrödinger-Poisson block
  - Iterative schemes
  - Solvers for Schrödinger and Poisson
- 3 Solvers for the BTE block
  - **Adimensionalizations**
  - Time discretization
  - Linear advection
  - PWENO interpolations
- 4 Experiments
  - Simplifying assumptions
  - Equilibria
  - Time-dependent simulations
  - Newton vs. Gummel
  - Plasma oscillations

# Wave-vector space

Two different adimensionalizations are proposed for the wave-vector space. Magnitudes with tilde are meant with dimension.

## Cartesian coordinates

$$(\tilde{k}_x, \tilde{k}_y) = \frac{\sqrt{m_e \kappa_B T_L}}{\hbar} (k_x, k_y).$$

## Ellipsoidal coordinated

The wave-vector for the  $\nu^{\text{th}}$  valley reads:

$$(\tilde{k}_x, \tilde{k}_y) = \frac{\sqrt{m_e \kappa_B T_L}}{\hbar} \sqrt{2w(1 + \alpha_\nu w)} (\sqrt{m_{x,\nu}} \cos(\phi), \sqrt{m_{y,\nu}} \sin(\phi)).$$

# Wave-vector space

Two different adimensionalizations are proposed for the wave-vector space. Magnitudes with tilde are meant with dimension.

## Cartesian coordinates

$$(\tilde{k}_x, \tilde{k}_y) = \frac{\sqrt{m_e \kappa_B T_L}}{\hbar} (k_x, k_y).$$

## Ellipsoidal coordinated

The wave-vector for the  $\nu^{\text{th}}$  valley reads:

$$(\tilde{k}_x, \tilde{k}_y) = \frac{\sqrt{m_e \kappa_B T_L}}{\hbar} \sqrt{2w(1 + \alpha_\nu w)} (\sqrt{m_{x,\nu}} \cos(\phi), \sqrt{m_{y,\nu}} \sin(\phi)).$$

# Wave-vector space

Two different adimensionalizations are proposed for the wave-vector space. Magnitudes with tilde are meant with dimension.

## Cartesian coordinates

$$(\tilde{k}_x, \tilde{k}_y) = \frac{\sqrt{m_e \kappa_B T_L}}{\hbar} (k_x, k_y).$$

## Ellipsoidal coordinated

The wave-vector for the  $\nu^{\text{th}}$  valley reads:

$$(\tilde{k}_x, \tilde{k}_y) = \frac{\sqrt{m_e \kappa_B T_L}}{\hbar} \sqrt{2w(1 + \alpha_\nu w)} (\sqrt{m_{x,\nu}} \cos(\phi), \sqrt{m_{y,\nu}} \sin(\phi)).$$

# BTE in cartesian coordinates

Let the flux coefficients

$$\begin{aligned} a_{\nu}^1(k) &= C^{\nu} v_{x,\nu}(k) \\ a_{\nu,p}^2(x) &= -C^{\nu} \frac{\partial e_{x,\nu}^{pot}}{\partial x}(x). \end{aligned}$$

Transport form

The BTE in transport form reads

$$\frac{\partial f_{\nu,p}}{\partial t} + a_{\nu}^1 \frac{\partial f_{\nu,p}}{\partial x} + a_{\nu,p}^2 \frac{\partial f_{\nu,p}}{\partial k} = \mathcal{Q}_{\nu,p}[f].$$

Conservation-law form

The BTE in conservation-law form reads

$$\frac{\partial f_{\nu,p}}{\partial t} + \frac{\partial}{\partial x} \left[ a_{\nu}^1 f_{\nu,p} \right] + \frac{\partial}{\partial k} \left[ a_{\nu,p}^2 f_{\nu,p} \right] = \mathcal{Q}_{\nu,p}[f].$$



# BTE in cartesian coordinates

Let the flux coefficients

$$\begin{aligned} a_{\nu}^1(k) &= C^{\nu} v_{x,\nu}(k) \\ a_{\nu,p}^2(x) &= -C^{\nu} \frac{\partial e_{x,\nu}^{pot}}{\partial x}(x). \end{aligned}$$

## Transport form

The BTE in transport form reads

$$\frac{\partial f_{\nu,p}}{\partial t} + a_{\nu}^1 \frac{\partial f_{\nu,p}}{\partial x} + a_{\nu,p}^2 \frac{\partial f_{\nu,p}}{\partial k} = \mathcal{Q}_{\nu,p}[f].$$

## Conservation-law form

The BTE in conservation-law form reads

$$\frac{\partial f_{\nu,p}}{\partial t} + \frac{\partial}{\partial x} [a_{\nu}^1 f_{\nu,p}] + \frac{\partial}{\partial k} [a_{\nu,p}^2 f_{\nu,p}] = \mathcal{Q}_{\nu,p}[f].$$

# BTE in cartesian coordinates

Let the flux coefficients

$$\begin{aligned} a_\nu^1(k) &= C^\nu v_{x,\nu}(k) \\ a_{\nu,p}^2(x) &= -C^\nu \frac{\partial e_{x,\nu}^{pot}}{\partial x}(x). \end{aligned}$$

## Transport form

The BTE in transport form reads

$$\frac{\partial f_{\nu,p}}{\partial t} + a_\nu^1 \frac{\partial f_{\nu,p}}{\partial x} + a_{\nu,p}^2 \frac{\partial f_{\nu,p}}{\partial k} = \mathcal{Q}_{\nu,p}[f].$$

## Conservation-law form

The BTE in conservation-law form reads

$$\frac{\partial f_{\nu,p}}{\partial t} + \frac{\partial}{\partial x} \left[ a_\nu^1 f_{\nu,p} \right] + \frac{\partial}{\partial k} \left[ a_{\nu,p}^2 f_{\nu,p} \right] = \mathcal{Q}_{\nu,p}[f].$$

# BTE in ellipsoidal coordinates

Let the flux coefficients

$$a_{\nu}^1(w, \phi) = C^{\nu} \frac{\sqrt{2w(1 + \alpha_{\nu}w)} \cos(\phi)}{\sqrt{m_{x,\nu}}} \frac{1}{1 + 2\alpha_{\nu}w}$$

$$a_{\nu,p}^2(x, w, \phi) = -C^{\nu} \frac{\partial \epsilon_{\nu,p}}{\partial x}(x) \frac{1}{1 + 2\alpha_{\nu}w} \frac{\sqrt{2w(1 + \alpha_{\nu}w)} \cos(\phi)}{\sqrt{m_{x,\nu}}}$$

$$a_{\nu,p}^3(x, w, \phi) = C^{\nu} \frac{\partial \epsilon_{\nu,p}}{\partial x}(x) \frac{\sin(\phi)}{\sqrt{m_{x,\nu}} \sqrt{2w(1 + \alpha_{\nu}w)}}.$$

Conservation-law form

$$\frac{\partial \Phi_{\nu,p}}{\partial t} + \frac{\partial}{\partial x} [a_{\nu}^1 \Phi_{\nu,p}] + \frac{\partial}{\partial w} [a_{\nu,p}^2 \Phi_{\nu,p}] + \frac{\partial}{\partial \phi} [a_{\nu,p}^3 \Phi_{\nu,p}] = \mathcal{Q}_{\nu,p}[\Phi]s(w)$$

# BTE in ellipsoidal coordinates

Let the flux coefficients

$$\begin{aligned}
 a_{\nu}^1(w, \phi) &= C^{\nu} \frac{\sqrt{2w(1 + \alpha_{\nu}w)} \cos(\phi)}{\sqrt{m_{x,\nu}}} \frac{1}{1 + 2\alpha_{\nu}w} \\
 a_{\nu,p}^2(x, w, \phi) &= -C^{\nu} \frac{\partial \epsilon_{\nu,p}}{\partial x}(x) \frac{1}{1 + 2\alpha_{\nu}w} \frac{\sqrt{2w(1 + \alpha_{\nu}w)} \cos(\phi)}{\sqrt{m_{x,\nu}}} \\
 a_{\nu,p}^3(x, w, \phi) &= C^{\nu} \frac{\partial \epsilon_{\nu,p}}{\partial x}(x) \frac{\sin(\phi)}{\sqrt{m_{x,\nu}} \sqrt{2w(1 + \alpha_{\nu}w)}}.
 \end{aligned}$$

Conservation-law form

$$\frac{\partial \Phi_{\nu,p}}{\partial t} + \frac{\partial}{\partial x} \left[ a_{\nu,p}^1 \Phi_{\nu,p} \right] + \frac{\partial}{\partial w} \left[ a_{\nu,p}^2 \Phi_{\nu,p} \right] + \frac{\partial}{\partial \phi} \left[ a_{\nu,p}^3 \Phi_{\nu,p} \right] = \mathcal{Q}_{\nu,p}[\Phi]s(w)$$

# Outline

- 1 The model
  - Geometry
  - Mathematical model
- 2 Numerical methods for the Schrödinger-Poisson block
  - Iterative schemes
  - Solvers for Schrödinger and Poisson
- 3 Solvers for the BTE block
  - Adimensionalizations
  - **Time discretization**
  - Linear advection
  - PWENO interpolations
- 4 Experiments
  - Simplifying assumptions
  - Equilibria
  - Time-dependent simulations
  - Newton vs. Gummel
  - Plasma oscillations

# Runge-Kutta vs. splitting

We propose two discretizations for the time, following the choice between conservation-law form and transport form.

## Runge-Kutta

If the BTE is written in conservation-law form, then we advance in time by the third order Total Variation Diminishing Runge-Kutta scheme: if the evolution equation

reads  $\frac{df}{dt} = H(t, f)$ , then

$$\textcircled{1} \quad f^{(1)} = \Delta t H^n(t^n, f^n)$$

$$\textcircled{2} \quad f^{(2)} = \frac{3}{4}f^n + \frac{1}{4}f^{(1)} + \frac{1}{4}\Delta t H^{(1)}(t^n + \Delta t, f^{(1)})$$

$$\textcircled{3} \quad f^{n+1} = \frac{1}{3}f^n + \frac{2}{3}f^{(2)} + \frac{2}{3}H^{(2)}\left(t^n + \frac{1}{2}\Delta t, f^{(2)}\right)$$

# Runge-Kutta vs. splitting

We propose two discretizations for the time, following the choice between conservation-law form and transport form.

## Runge-Kutta

If the BTE is written in conservation-law form, then we advance in time by the third order Total Variation Diminishing Runge-Kutta scheme: if the evolution equation

reads  $\frac{df}{dt} = H(t, f)$ , then

$$\textcircled{1} \quad f^{(1)} = \Delta t H^n(t^n, f^n)$$

$$\textcircled{2} \quad f^{(2)} = \frac{3}{4}f^n + \frac{1}{4}f^{(1)} + \frac{1}{4}\Delta t H^{(1)}(t^n + \Delta t, f^{(1)})$$

$$\textcircled{3} \quad f^{n+1} = \frac{1}{3}f^n + \frac{2}{3}f^{(2)} + \frac{2}{3}H^{(2)}\left(t^n + \frac{1}{2}\Delta t, f^{(2)}\right)$$

# Splitting schemes

## Time splitting

If the BTE is written in transport form, then we advance in time by time splitting schemes:

$$\begin{aligned} \frac{\partial f_{\nu,p}}{\partial t} + C^{\nu} \{ \epsilon^{tot}, f_{\nu,p} \} &= 0 \\ \frac{\partial f_{\nu,p}}{\partial t} &= \mathcal{Q}_{\nu,p}[f]. \end{aligned}$$







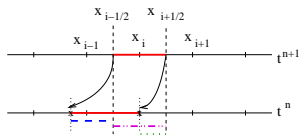
# Outline

- 1 The model
  - Geometry
  - Mathematical model
- 2 Numerical methods for the Schrödinger-Poisson block
  - Iterative schemes
  - Solvers for Schrödinger and Poisson
- 3 Solvers for the BTE block
  - Adimensionalizations
  - Time discretization
  - **Linear advection**
  - PWENO interpolations
- 4 Experiments
  - Simplifying assumptions
  - Equilibria
  - Time-dependent simulations
  - Newton vs. Gummel
  - Plasma oscillations

# Linear advection

## Flux Balance Method:

Total mass conservation is forced. It is based on the idea of following backward the characteristics, but integral values are taken instead of point values:



— The averages along the red segments are the same, because we have followed the characteristics backward.

FLUX BALANCE METHOD means evaluating the flux at time  $t^{n+1}$  from a balance of fluxes at previous time  $t^n$  :

— the average along the purple segment

- - - plus the average along the blue segment

..... minus the average along the green segment

# Outline

- 1 The model
  - Geometry
  - Mathematical model
- 2 Numerical methods for the Schrödinger-Poisson block
  - Iterative schemes
  - Solvers for Schrödinger and Poisson
- 3 **Solvers for the BTE block**
  - Adimensionalizations
  - Time discretization
  - Linear advection
  - **PWENO interpolations**
- 4 Experiments
  - Simplifying assumptions
  - Equilibria
  - Time-dependent simulations
  - Newton vs. Gummel
  - Plasma oscillations

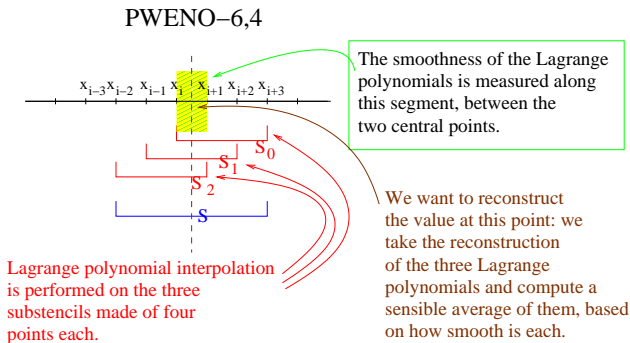




# Non-oscillatory properties

Essentially Non Oscillatory (ENO) methods are based on on a sensible average of Lagrange polynomial reconstructions.

We describe the case of PWENO-6,4: we take a stencil of six points and divide it into three substencils of four points:







# The average

If we note  $p_r(x)$  the Lagrange polynomials, PWENO reconstruction reads

$$p_{PWENO}(x) = \omega_0(x)p_0(x) + \omega_1(x)p_1(x) + \omega_2(x)p_2(x).$$

Convex combination.

The convex combination  $\{\omega_r(x)\}_r$  must penalize the substencils  $\mathcal{S}_r$  in which the  $p_r(x)$  have high derivatives.

Smoothness indicators

In order to decide which substencils  $\mathcal{S}_r$  are “regular” and which ones are not, we have to introduce the smoothness indicators: we use a weighted sum of the  $L^2$ -norms of the Lagrange polynomials  $p_r(x)$  to measure their regularity close to the reconstruction point  $x$ . The following smoothness indicators have been proposed by Jiang and Shu:

$$\beta_r = \Delta x \left\| \frac{dp_r}{dx} \right\|_{L^2_{(x_i, x_{i+1})}} + \Delta x^3 \left\| \frac{d^2 p_r}{dx^2} \right\|_{L^2_{(x_i, x_{i+1})}} + \Delta x^5 \left\| \frac{d^3 p_r}{dx^3} \right\|_{L^2_{(x_i, x_{i+1})}}.$$

# The average

If we note  $p_r(x)$  the Lagrange polynomials, PWENO reconstruction reads

$$p_{PWENO}(x) = \omega_0(x)p_0(x) + \omega_1(x)p_1(x) + \omega_2(x)p_2(x).$$

## Convex combination.

The convex combination  $\{\omega_r(x)\}_r$  must penalize the substencils  $\mathcal{S}_r$  in which the  $p_r(x)$  have high derivatives.

## Smoothness indicators

In order to decide which substencils  $\mathcal{S}_r$  are “regular” and which ones are not, we have to introduce the smoothness indicators: we use a weighted sum of the  $L^2$ -norms of the Lagrange polynomials  $p_r(x)$  to measure their regularity close to the reconstruction point  $x$ . The following smoothness indicators have been proposed by Jiang and Shu:

$$\beta_r = \Delta x \left\| \frac{dp_r}{dx} \right\|_{L^2_{(x_i, x_{i+1})}} + \Delta x^3 \left\| \frac{d^2 p_r}{dx^2} \right\|_{L^2_{(x_i, x_{i+1})}} + \Delta x^5 \left\| \frac{d^3 p_r}{dx^3} \right\|_{L^2_{(x_i, x_{i+1})}}.$$

# The average

If we note  $p_r(x)$  the Lagrange polynomials, PWENO reconstruction reads

$$p_{PWENO}(x) = \omega_0(x)p_0(x) + \omega_1(x)p_1(x) + \omega_2(x)p_2(x).$$

## Convex combination.

The convex combination  $\{\omega_r(x)\}_r$  must penalize the substencils  $\mathcal{S}_r$  in which the  $p_r(x)$  have high derivatives.

## Smoothness indicators

In order to decide which substencils  $\mathcal{S}_r$  are “regular” and which ones are not, we have to introduce the smoothness indicators: we use a weighted sum of the  $L^2$ -norms of the Lagrange polynomials  $p_r(x)$  to measure their regularity close to the reconstruction point  $x$ . The following smoothness indicators have been proposed by Jiang and Shu:

$$\beta_r = \Delta x \left\| \frac{dp_r}{dx} \right\|_{L^2_{(x_i, x_{i+1})}} + \Delta x^3 \left\| \frac{d^2 p_r}{dx^2} \right\|_{L^2_{(x_i, x_{i+1})}} + \Delta x^5 \left\| \frac{d^3 p_r}{dx^3} \right\|_{L^2_{(x_i, x_{i+1})}}.$$

# High order reconstruction

Admit for now that the convex combination is given by the normalization

$\omega_r(x) = \frac{\tilde{\omega}_r(x)}{\sum_{s=0}^2 \tilde{\omega}_s(x)}$  of the protoweights  $\tilde{\omega}_r(x)$  defined this way:

$$\tilde{\omega}_r(x) = \frac{d_r(x)}{(\epsilon + \beta_r)^2}.$$

## Regular reconstruction

Suppose that all the  $\beta_r$  are equal; then we have

$$\omega_r(x) = d_r(x).$$

The optimal order is achieved by Lagrange reconstruction  $p_{Lagrange}(x)$  in the whole stencil  $\mathcal{S}$ , so if we define  $d_r(x)$  to be the polynomials such that

$$p_{Lagrange}(x) = d_0(x)p_0(x) + d_1(x)p_1(x) + d_2(x)p_2(x),$$

then we have achieved the optimal order because  $p_{PWENO}(x) = p_{Lagrange}(x)$ .

# High order reconstruction

Admit for now that the convex combination is given by the normalization

$\omega_r(x) = \frac{\tilde{\omega}_r(x)}{\sum_{s=0}^2 \tilde{\omega}_s(x)}$  of the protoweights  $\tilde{\omega}_r(x)$  defined this way:

$$\tilde{\omega}_r(x) = \frac{d_r(x)}{(\epsilon + \beta_r)^2}.$$

## Regular reconstruction

Suppose that all the  $\beta_r$  are equal; then we have

$$\omega_r(x) = d_r(x).$$

The optimal order is achieved by Lagrange reconstruction  $p_{Lagrange}(x)$  in the whole stencil  $\mathcal{S}$ , so if we define  $d_r(x)$  to be the polynomials such that

$$p_{Lagrange}(x) = d_0(x)p_0(x) + d_1(x)p_1(x) + d_2(x)p_2(x),$$

then we have achieved the optimal order because  $p_{PWENO}(x) = p_{Lagrange}(x)$ .

# High order reconstruction

Admit for now that the convex combination is given by the normalization

$\omega_r(x) = \frac{\tilde{\omega}_r(x)}{\sum_{s=0}^2 \tilde{\omega}_s(x)}$  of the protoweights  $\tilde{\omega}_r(x)$  defined this way:

$$\tilde{\omega}_r(x) = \frac{d_r(x)}{(\epsilon + \beta_r)^2}.$$

## High gradients

Otherwise, suppose for instance that  $\beta_0$  is high order than the other ones: in this case  $S_0$  is penalized and most of the reconstruction is carried by the other more “regular” substencils.

# Outline

- 1 The model
  - Geometry
  - Mathematical model
- 2 Numerical methods for the Schrödinger-Poisson block
  - Iterative schemes
  - Solvers for Schrödinger and Poisson
- 3 Solvers for the BTE block
  - Adimensionalizations
  - Time discretization
  - Linear advection
  - PWENO interpolations
- 4 Experiments
  - **Simplifying assumptions**
  - Equilibria
  - Time-dependent simulations
  - Newton vs. Gummel
  - Plasma oscillations



# Collision operator

Results are presented for the the DG MOSFET in the one-valley, parabolic-band approximation. Moreover, the complete collision operator is substituted by a simple relaxation-time operator:

$$\mathcal{Q}_p f = \frac{1}{\tau} (\rho_p M - f_p).$$

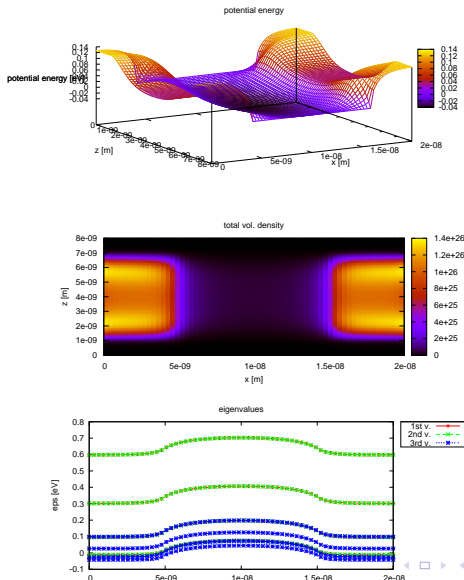
The goal of this work is just the setting up of numerical tools for a more profound and realistic simulation.

A parallel code in the most realistic case is being implemented.

# Outline

- 1 The model
  - Geometry
  - Mathematical model
- 2 Numerical methods for the Schrödinger-Poisson block
  - Iterative schemes
  - Solvers for Schrödinger and Poisson
- 3 Solvers for the BTE block
  - Adimensionalizations
  - Time discretization
  - Linear advection
  - PWENO interpolations
- 4 Experiments
  - Simplifying assumptions
  - **Equilibria**
  - Time-dependent simulations
  - Newton vs. Gummel
  - Plasma oscillations

# Thermodynamical equilibrium: three-valley case



# Outline

- 1 The model
  - Geometry
  - Mathematical model
- 2 Numerical methods for the Schrödinger-Poisson block
  - Iterative schemes
  - Solvers for Schrödinger and Poisson
- 3 Solvers for the BTE block
  - Adimensionalizations
  - Time discretization
  - Linear advection
  - PWENO interpolations
- 4 Experiments
  - Simplifying assumptions
  - Equilibria
  - **Time-dependent simulations**
  - Newton vs. Gummel
  - Plasma oscillations

# Long-time behavior

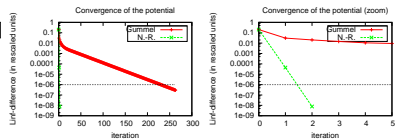
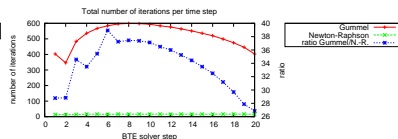
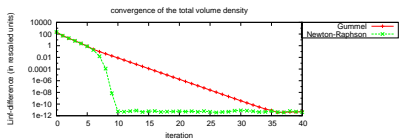
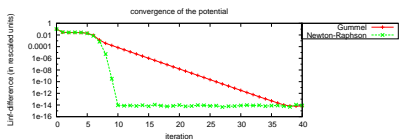
We propose now some results relative to the long-time behavior of the system.

# Outline

- 1 The model
  - Geometry
  - Mathematical model
- 2 Numerical methods for the Schrödinger-Poisson block
  - Iterative schemes
  - Solvers for Schrödinger and Poisson
- 3 Solvers for the BTE block
  - Adimensionalizations
  - Time discretization
  - Linear advection
  - PWENO interpolations
- 4 Experiments
  - Simplifying assumptions
  - Equilibria
  - Time-dependent simulations
  - **Newton vs. Gummel**
  - Plasma oscillations

# Number of iterations

Newton schemes require much less iterations than Gummel in order to compute the thermodynamical equilibrium.

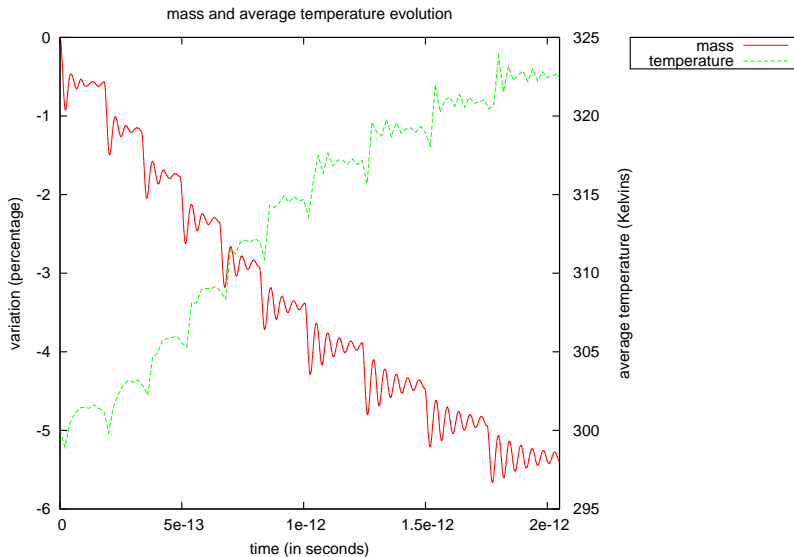


# Outline

- 1 The model
  - Geometry
  - Mathematical model
- 2 Numerical methods for the Schrödinger-Poisson block
  - Iterative schemes
  - Solvers for Schrödinger and Poisson
- 3 Solvers for the BTE block
  - Adimensionalizations
  - Time discretization
  - Linear advection
  - PWENO interpolations
- 4 Experiments
  - Simplifying assumptions
  - Equilibria
  - Time-dependent simulations
  - Newton vs. Gummel
  - Plasma oscillations



# Mass and temperature oscillations



# Numerically-computed oscillations

The plasma frequency is given by

$$\omega_p = \sqrt{\frac{q^2 N_e}{\epsilon_R \epsilon_0 m_*}}$$

$N_D^{high}$ ( $\times 10^{26} m^{-3}$ )	$\epsilon_R$	$m_*$	$N_e$ ( $\times 10^{26} m^{-3}$ )	$\omega_{num}$ ( $\times 10^{14} s^{-1}$ )	$\omega_p$ ( $\times 10^{14} s^{-1}$ )	Ratio $\frac{\omega_{num}}{\omega_{ref}}$	Expected Ratio
1	11.7	0.5	.400	$\omega_{ref} = 1.344$	1.475	1	/
2	11.7	0.5	.783	2.051	2.064	1.52	$\sqrt{2}$
4	11.7	0.5	1.544	2.813	2.899	2.09	2
1	5.85	0.5	.400	1.848	2.086	1.37	$\sqrt{2}$